

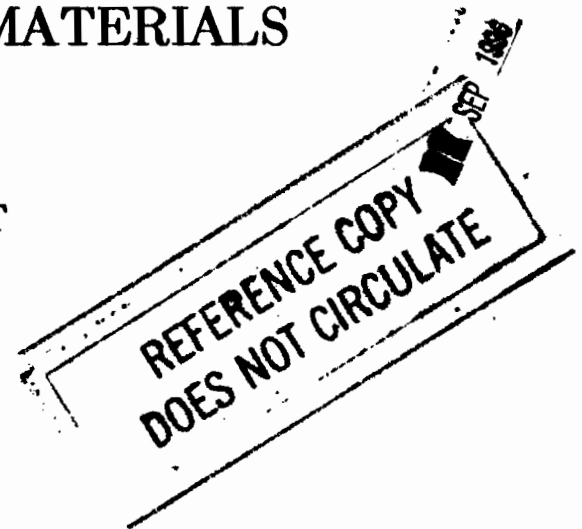
  
AD

MEMORANDUM REPORT BRL-MR-3569

**ADIABATIC SHEAR BANDS IN SIMPLE  
AND DIPOLAR PLASTIC MATERIALS**

**THOMAS W. WRIGHT  
ROMESH C. BATRA**

**MARCH 1987**



APPROVED FOR PUBLIC RELEASE; DISTRIBUTION UNLIMITED.

**US ARMY BALLISTIC RESEARCH LABORATORY  
ABERDEEN PROVING GROUND, MARYLAND**

Destroy this report when it is no longer needed.  
Do not return it to the originator.

Additional copies of this report may be obtained  
from the National Technical Information Service,  
U. S. Department of Commerce, Springfield, Virginia  
22161.

The findings in this report are not to be construed as an official  
Department of the Army position, unless so designated by other  
authorized documents.

The use of trade names or manufacturers' names in this report  
does not constitute indorsement of any commercial product.

UNCLASSIFIED

SECURITY CLASSIFICATION OF THIS PAGE

## REPORT DOCUMENTATION PAGE

Form Approved  
OMB No. 0704-0188  
Exp. Date: Jun 30, 1986

1a. REPORT SECURITY CLASSIFICATION Unclassified			1b. RESTRICTIVE MARKINGS	
2a. SECURITY CLASSIFICATION AUTHORITY			3. DISTRIBUTION/AVAILABILITY OF REPORT Approved for public release; distribution unlimited	
2b. DECLASSIFICATION/DOWNGRADING SCHEDULE				
4. PERFORMING ORGANIZATION REPORT NUMBER(S)			5. MONITORING ORGANIZATION REPORT NUMBER(S)	
6a. NAME OF PERFORMING ORGANIZATION US Army Ballistic Research Laboratory		6b. OFFICE SYMBOL (If applicable) SLCBB-TB-S	7a. NAME OF MONITORING ORGANIZATION	
6c. ADDRESS (City, State, and ZIP Code) Aberdeen Proving Ground, Maryland 21005-5066			7b. ADDRESS (City, State, and ZIP Code)	
8a. NAME OF FUNDING/SPONSORING ORGANIZATION		8b. OFFICE SYMBOL (If applicable)	9. PROCUREMENT INSTRUMENT IDENTIFICATION NUMBER	
8c. ADDRESS (City, State, and ZIP Code)			10. SOURCE OF FUNDING NUMBERS	
			PROGRAM ELEMENT NO.	PROJECT NO.
			TASK NO.	WORK UNIT ACCESSION NO.
11. TITLE (Include Security Classification) Adiabatic Shear Bands in Simple and Dipolar Plastic Materials				
12. PERSONAL AUTHOR(S) Wright, Thomas W.; Batra, Romesh C. (University of Missouri-Rolla)				
13a. TYPE OF REPORT		13b. TIME COVERED FROM _____ TO _____		14. DATE OF REPORT (Year, Month, Day)
15. PAGE COUNT				
16. SUPPLEMENTARY NOTATION				
17. COSATI CODES			18. SUBJECT TERMS (Continue on reverse if necessary and identify by block number) Shear bands, Viscoplasticity, High rate deformation	
FIELD	GROUP	SUB-GROUP		
19. ABSTRACT (Continue on reverse if necessary and identify by block number) A simple version of thermo/viscoplasticity is used to model the formation of adiabatic shear bands in high rate deformation of solids. The one-dimensional shearing deformation of a finite slab is considered. Equations are formulated and numerical solutions are found for dipolar plastic materials. These solutions are contrasted and compared with previous solutions for simple materials.				
20. DISTRIBUTION/AVAILABILITY OF ABSTRACT <input type="checkbox"/> UNCLASSIFIED/UNLIMITED <input type="checkbox"/> SAME AS RPT. <input type="checkbox"/> DTIC USERS			21. ABSTRACT SECURITY CLASSIFICATION Unclassified	
22a. NAME OF RESPONSIBLE INDIVIDUAL Thomas W. Wright			22b. TELEPHONE (Include Area Code) (301) 278-6046	22c. OFFICE SYMBOL SLCBB-TB-S

## TABLE OF CONTENTS

	<u>Page</u>
LIST OF ILLUSTRATIONS. . . . .	v
I. INTRODUCTION . . . . .	7
II. FORMULATION OF THE PROBLEM . . . . .	7
III. CONSTITUTIVE EQUATIONS AND NONDIMENSIONAL FORMS . . . . .	9
IV. HOMOGENEOUS SOLUTIONS AND PERTURBATIONS . . . . .	11
V. DISCUSSION AND CONCLUSIONS . . . . .	17
REFERENCES . . . . .	21
DISTRIBUTION LIST . . . . .	23

# LIST OF ILLUSTRATIONS

<u>FIG.</u>		<u>Page</u>
1	Typical reference, isothermal, and adiabatic response curves. . . .	13
2	Plastic strain rate in the center of the band with a temperature perturbation. . . . .	14
3	Cross plots of plastic strain for increasing deformation. . . . .	16
4	Cross plots of dipolar stress for increasing deformation. . . . .	18
5	Stress in a shear band. . . . .	19

## I. INTRODUCTION

Adiabatic shear is the name given to a localization phenomenon that occurs during high rate plastic deformation such as machining, explosive forming, shock impact loading, or ballistic penetration. The process is usually described as being initiated by thermal softening in competition with rate effects and work hardening. Heat generated by plastic work softens the material so that eventually stress falls with increasing strain. When that occurs, the material becomes unstable locally and tends to accumulate essentially all of any additional imposed strain in a narrow band. In turn the local heating increases, and the process is driven further. As the localization intensifies, substantial gradients of temperature build up so that in the later stages of development heat flows out of the band thus tending to offset the thermal buildup in the band.

In two previous papers Wright and Batra<sup>1,2</sup> have described the results of computations that simulate the formation of a single shear band from a local temperature inhomogeneity in a simple material. Strain gradients in the calculations reach approximately 0.2 per  $\mu\text{m}$ , and experimental evidence<sup>3</sup> indicates gradients that ultimately are orders of magnitude larger. Therefore, it has seemed worthwhile to reformulate the theory to include gradient effects. This has been accomplished by modifying the dipolar theory due to Green, McInnis, and Naghdi<sup>4</sup> to include a rate effect.

## II. FORMULATION OF THE PROBLEM

In order to concentrate on fundamentals, the process has been idealized as one dimensional shearing of a finite block of material. Accordingly the three dimensional theory of Green, et al<sup>4</sup> is summarized here for one dimension. In addition, the yield function is taken to depend on the plastic parts of strain rate and gradient of strain rate as well as the usual variables.

A one dimensional shearing motion can be expressed as

$$x = X + u(Y, t), \quad y = Y, \quad z = Z \quad \text{for } -H \leq Y \leq +H \quad (1)$$

If it is supposed that on any fixed surface  $Y$  is constant, surface tractions,  $\tau$ , do work against the velocity,  $\dot{x}$ , and hypertractions,  $\sigma$ , do work against the velocity gradient,  $\dot{x}_{,Y}$ , then the one dimensional expressions for balance of linear momentum, energy, and entropy may be written as equations (2).

$$\tau_{,Y} + \hat{\rho}b = \rho\ddot{x}$$

$$\rho\dot{U} = \tau\dot{x}_{,Y} + (\sigma\dot{x}_{,Y}),_Y - q_{,Y} + \rho(\hat{c}\dot{x}_{,Y} + r) \quad (2)$$

$$\rho T\dot{\eta} - \frac{q}{T} T_{,Y} + q_{,Y} - \rho r \geq 0$$

In these equations  $\hat{b}$  and  $\hat{c}$  are the simple and dipolar body forces respectively,  $U$  is the internal energy,  $q$  is heat flux,  $r$  is the volumetric supply of energy,  $T$  is temperature,  $\eta$  is specific entropy, and  $\rho$  is mass density, which is constant. The superimposed dot and the comma followed by  $Y$  indicate differentiation with respect to time  $t$  and the material coordinate,  $Y$ , respectively. Following Green, et al,<sup>4</sup> it will be convenient to define another stress by the equation

$$s \equiv \tau + \sigma_{,Y} + \rho \hat{c} \quad (3)$$

Equations (2) hold for any dipolar material, either elastic or plastic, for motions of the type given by (1).

Now define shear strain and shear strain gradient by

$$\gamma \equiv x_{,Y} \quad d \equiv \gamma_{,Y} = x_{,YY}$$

and suppose that these can both be decomposed into elastic and plastic parts.

$$\gamma = \gamma_e + \gamma_p, \quad d = d_e + d_p \quad (4)$$

None of  $\gamma_e$ ,  $\gamma_p$ ,  $d_e$  or  $d_p$  are necessarily gradients, but of course their sums  $\gamma$  and  $d$  must be the gradients of  $x$  and  $\gamma$ , respectively. Next let  $\kappa$  be a measure of plastic work hardening. Finally, in the same spirit as classical plasticity, a scalar yield or loading function  $f$  is assumed to exist, but here it is taken to depend on plastic strain rates, as well as stresses and temperature,

$$f(s, \sigma, T, \dot{\gamma}_p, \dot{d}_p) = \kappa \quad (5)$$

In general this and other plastic constitutive functions could depend on elastic and plastic strains as well, but that possibility will be ignored in this paper unless explicitly stated otherwise.

The static yield surface is given by (5) with  $\dot{\gamma}_p = \dot{d}_p = 0$ , and for quasi-static deformations a continuity argument for neutral loading, as advanced in Ref. 4 leads to the following reduced forms for the plastic rates.

$$\dot{\gamma}_p = \Lambda \alpha, \quad \dot{d}_p = \Lambda \beta \quad (6)$$

where  $\alpha$  and  $\beta$  are constitutive functions that depend only on  $s$ ,  $\sigma$ ,  $T$ , and  $\kappa$ .

The multiplier  $\Lambda$  is proportional to  $\hat{f} = f_s \dot{s} + f_\sigma \dot{\sigma} + f_T \dot{T}$ , where the subscripts

denote partial differentiation with respect to the arguments, and  $\dot{\gamma}_p = \dot{d}_p = 0$  in evaluating the derivatives of  $f$ .

Now let it be assumed that (6) holds even when  $\dot{\gamma}_p \neq 0$ ,  $\dot{d}_p \neq 0$ , so that in the general case (5) becomes

$$f(s, \sigma, T, \Lambda\alpha(s, \sigma, T, \kappa), \Lambda\beta(s, \sigma, T, \kappa)) = \kappa \quad (7)$$

and the criterion for elastic or plastic loading is simply

$$\begin{aligned} f(s, \sigma, T, 0, 0) &\leq \kappa, \text{ elastic;} \\ f(s, \sigma, T, 0, 0) &> \kappa, \text{ plastic.} \end{aligned} \quad (8)$$

To make sense the derivative  $f_\Lambda$ , obtained from (7) must be negative for all values of the other arguments. Then if plastic flow is occurring according to (8),  $\Lambda$  may be found from inversion of (7), and because of the assumed monotonicity of  $f$  with respect to  $\Lambda$ , there will always be a unique solution with  $\Lambda > 0$ . With the assumption that  $U, s, \sigma, T$  depend on the variables  $\gamma_e, d_e, \eta$  and that  $q$  depends on the same variables plus the gradient  $T_{,Y}$ , standard thermodynamic arguments give

$$T = \frac{\partial U}{\partial \eta}, \quad s = \rho \frac{\partial U}{\partial \gamma_e}, \quad \sigma = \rho \frac{\partial U}{\partial d_e} \quad (9)$$

The energy and entropy laws now reduce to

$$\rho T \dot{\eta} = s \dot{\gamma}_p + \sigma \dot{d}_p - q_{,Y} + \rho r, \quad s \dot{\gamma}_p + \sigma \dot{d}_p - \frac{q}{T_{,Y}} \geq 0 \quad (10)$$

where  $\dot{\gamma}_p = \dot{d}_p = 0$  during elastic deformation and  $\neq 0$  during plastic deformation.

### III. CONSTITUTIVE EQUATIONS AND NONDIMENSIONAL FORMS

For computational purposes simple constitutive equations have been chosen as follows:

$$\begin{aligned} \rho U &= \frac{1}{2} \mu \gamma_e^2 + \frac{1}{2} \ell^2 \mu d_e^2 + \rho T_0 c \left( e^{\frac{\eta - \eta_0}{c}} - 1 \right) \\ \dot{\kappa} &= \frac{h(\kappa)}{\kappa} (s \dot{\gamma}_p + \sigma \dot{d}_p), \quad q = -k T_{,Y} \end{aligned} \quad (11)$$



$$\alpha = s, \quad \beta = \frac{1}{\ell} \sigma \quad (11 \text{ cont.})$$

$$(s^2 + \frac{1}{\ell} \sigma^2)^{1/2} = \kappa \{1 - a(T - T_0)\} \{1 + b(\dot{\gamma}_p^2 + \ell^2 \dot{d}_p^2)^{1/2}\}^m.$$

In (11)<sub>1</sub>  $\mu$  is the usual elastic shear modulus and  $\ell$  is a characteristic material property with the dimensions of length,  $T_0$  is a reference temperature, and  $c$  is specific heat. With this simple choice for the internal energy there is no thermoelastic effect and no thermal expansion. The stresses and the temperature follow from (9). In (11)<sub>2</sub> the function  $h(\kappa)$  is the plastic slope of a reference isothermal shear test, which is chosen to be

$$h = \frac{n}{\psi_0} \kappa_0^{\frac{1}{n}} \kappa^{1 - \frac{1}{n}} \quad (12)$$

Here  $\kappa_0$  is the initial yield stress,  $n$  is the work hardening exponent, and  $\psi_0$  may be chosen to fit the initial slope of an empirical curve of stress versus plastic strain. Equation (11)<sub>2</sub> states that  $\kappa$  evolves according to the plastic work done no matter what the conditions of the test. Equation (11)<sub>3</sub> is Fourier's law and equations (11)<sub>4</sub> and (11)<sub>5</sub> have been chosen in a simple form that is dimensionally correct and leads to positive plastic work. Finally in (11)<sub>6</sub> the function  $f$  has been chosen to be made up of three multiplicative factors involving the stresses, the temperature, and the plastic rates, respectively. In (11)<sub>6</sub>  $a$  is the coefficient of thermal softening,  $b$  is a characteristic time, and  $m$  is the strain rate exponent. In general the value of  $\ell$  could be different in each of the four places that it appears in (11), but such complexity is not warranted for the time being since there is no microscopic theory available for guidance.

In nondimensional form the full set of equations in the absence of body forces and supply of energy may be written as follows

$$\begin{aligned} \text{Momentum: } (s - \ell \sigma, \gamma), \gamma &= \rho v \\ \text{Energy: } \dot{\theta} &= k \theta, \gamma \gamma + s \dot{\gamma}_p + \ell \sigma \dot{d}_p \\ \text{Constitutive: } \dot{s} &= \mu(v, \gamma - \gamma_p), \quad \dot{\gamma}_p = \Lambda s \end{aligned} \quad (13)$$

$$\dot{\sigma} = \ell \mu (v, \dot{\gamma} \dot{\gamma} - \dot{d}_p), \quad \dot{d}_p = \frac{\Lambda}{\bar{\ell}} \sigma$$

$$\dot{\kappa} = \frac{h(\kappa)}{\bar{\kappa}} (s \dot{\gamma}_p + \ell \sigma \dot{d}_p), \quad h = \frac{n}{\psi_0} \kappa^1 - \frac{1}{n}$$

(13 cont.)

$$\text{Yield: } (s^2 + \sigma^2)^{1/2} = (1 - a\theta) \{1 + b\Lambda(s^2 + \sigma^2)^{1/2}\}^m$$

$$\text{where } \Lambda > 0 \text{ only if } (s^2 + \sigma^2)^{1/2} > \kappa(1 - a\theta)$$

$$\Lambda = 0 \text{ otherwise}$$

In (13) the temperature  $T$  has been replaced by the temperature increase  $\theta = T - T_0$ . The nondimensional variables are related to their dimensional (barred) counterparts as follows:

$$Y = \bar{Y}/H, \quad t = \bar{t}\dot{\gamma}_0$$

$$v = \bar{v}/H\dot{\gamma}_0, \quad s = \bar{s}/\kappa_0, \quad \sigma = \bar{\sigma}/\bar{\ell}\kappa_0, \quad \theta = \bar{\theta}\bar{\rho}c/\kappa_0, \quad \kappa = \bar{\kappa}/\kappa_0 \quad (14)$$

$$\gamma = \bar{\gamma}, \quad d = \bar{d}H, \quad \dot{\gamma}_p = \dot{\bar{\gamma}}_p/\dot{\gamma}_0, \quad \dot{d}_p = \dot{\bar{d}}_p H/\dot{\gamma}_0, \quad \Lambda = \bar{\Lambda} \kappa_0/\dot{\gamma}_0$$

Besides  $m$ ,  $n$ , and  $\psi_0$  there are six other nondimensional parameters, which are related to their dimensional (barred) counterparts as follows:

$$a = \bar{a}\kappa_0/\bar{\rho}c, \quad b = \bar{b}\dot{\gamma}_0, \quad k = \bar{k}/\bar{\rho}c\dot{\gamma}_0 H^2, \quad \ell = \bar{\ell}/H$$

(15)

$$\mu = \bar{\mu}/\kappa_0, \quad \rho = \bar{\rho}H^2\dot{\gamma}_0^2/\kappa_0$$

In (14) and (15)  $\dot{\gamma}_0 = \bar{v}(H, \bar{t})/H$  is the average applied strain rate between the boundaries  $\bar{Y} = \pm H$ .

#### IV. HOMOGENEOUS SOLUTIONS AND PERTURBATIONS

Equations (13) have homogeneous solutions with  $v = Y$  and all other dependent variables independent of  $Y$ . With initial values taken to be  $s(0) = \kappa(0) = 1$  and  $\theta(0) = \sigma(0) = 0$ , the solution for  $s$ ,  $\kappa$ , and  $\theta$  is exactly the same

as for a simple material (see Wright and Batra<sup>1,2</sup>) and  $\sigma$  is identically zero. Figure 1 shows several curves for homogeneous solutions of equations (13) obtained for particular choices of the parameters. With  $a = b = 0$  there is no thermal softening and no rate effect so the resulting curve is simply the slow, isothermal stress/strain curve, called the reference curve, from which the function  $h(\cdot)$  was derived. With  $a = 0$ , but with a finite value for  $b$ , the curve shows the isothermal response at a high rate of deformation. With finite values for both  $a$  and  $b$  the curve shows the adiabatic response at a high rate of deformation. The nondimensional parameters chosen here are the same as those listed in Ref. 2 namely

$$\begin{array}{llll} \rho = 3.928 \times 10^{-5} & k = 3.978 \times 10^{-3} & a = 0.4973 & \mu = 240.3 \\ n = 0.09 & \psi_0 = 0.017 & b = 5 \times 10^6 & m = 0.025 \end{array}$$

The value for  $\ell$  is immaterial for the homogeneous response as are  $\rho$  and  $k$ . The adiabatic response curve is typical. Initially the stress rises elastically above the reference curve, but as the overstress increases, plastic straining sets in, the temperature rises, and the response softens relative to the isothermal response. Eventually thermal softening wins over work and rate hardening, so that the stress passes through a maximum (indicated by P in the figure) and then decreases with further deformation. The general character of the homogeneous response is well understood and has been reported many times in the literature, although the way the response changes with the various parameters depends on the particular model used for the thermo/viscoplasticity.

Once peak stress has been passed the material becomes extremely sensitive to inhomogeneities, and the deformation has a strong tendency to localize. To examine this behavior for a dipolar material and to compare the results to previous calculations for a simple material, calculations have been made for the response following a small temperature perturbation. At the point marked I in Figure 1 the computed homogeneous response was modified by adding a smooth temperature bump (height 0.1 and width 0.5) to the basic homogeneous response. After recalculating  $s$  so that the yield condition in (13) is still satisfied with the new temperature distribution, the problem was restarted as a new initial-boundary value problem with all other initial values as calculated previously and with boundary values at  $Y = +1, 0$  taken to be  $v = 1, 0$  and  $\sigma = 0, \psi_Y = 0, 0$ . With these boundary values, the average strain rate in the strip is the same as in the homogeneous calculation and the material remains adiabatic overall. The same approach was used in Refs. 1 and 2 for a simple material, but now the new material parameter  $\ell$  is nonzero. Computations have been made for  $\ell = 0, 10^{-4}$  and  $10^{-2}$ . After casting the equations into a weak form, solutions were found using the finite element method for spatial discretization and an implicit Crank-Nicolson scheme to march forward in time. Previously a forward difference method was used for the time integration<sup>1,2</sup>, but the step size was necessarily very small for the dipolar case.

Typical results are shown in Figures 2, 3, 4 and 5. Figure 2 shows the plastic strain rate in the center of the band as a function of the average applied strain. The nondimensionalization is such that increments of time are

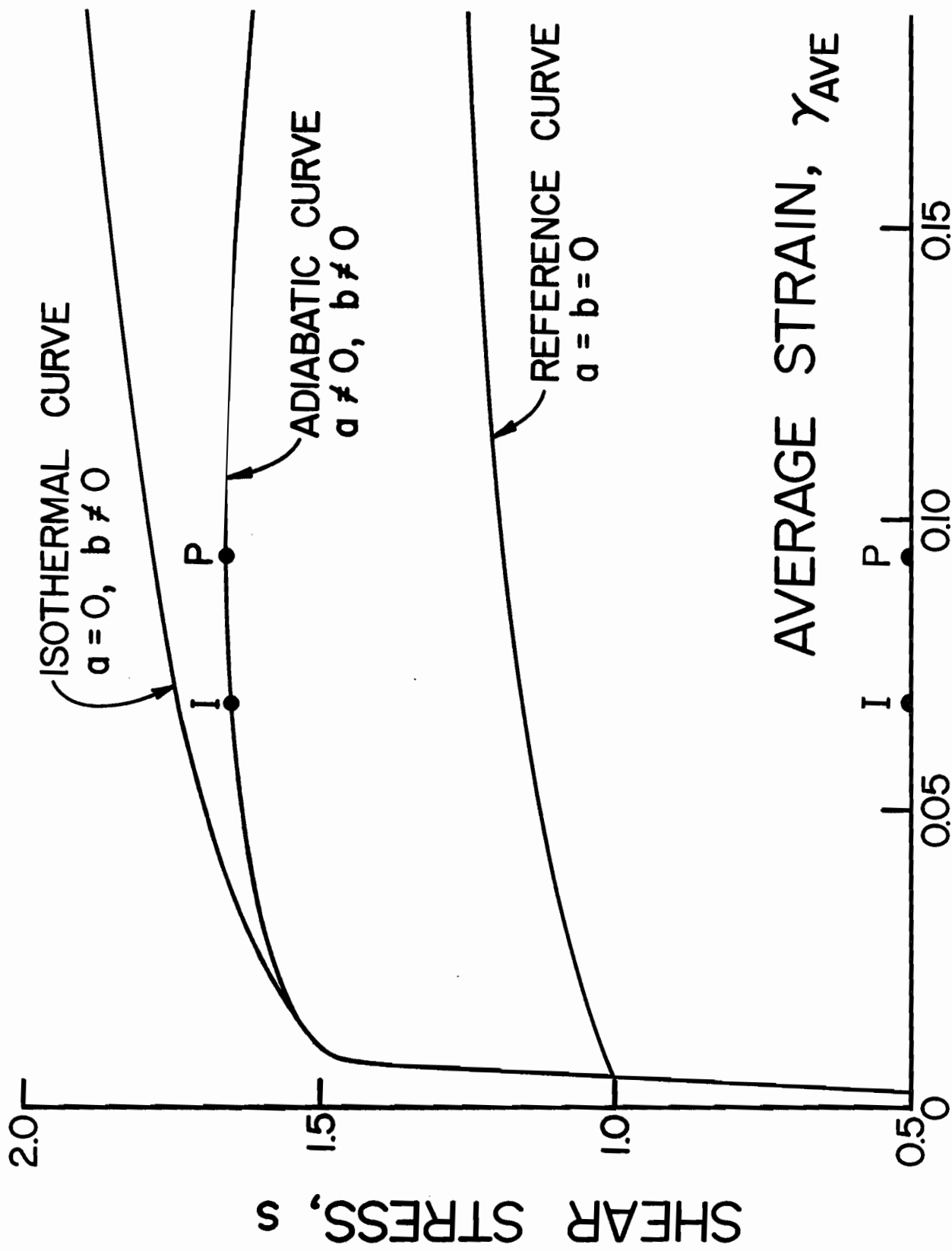


Figure 1. Typical reference, isothermal, and adiabatic response curves.

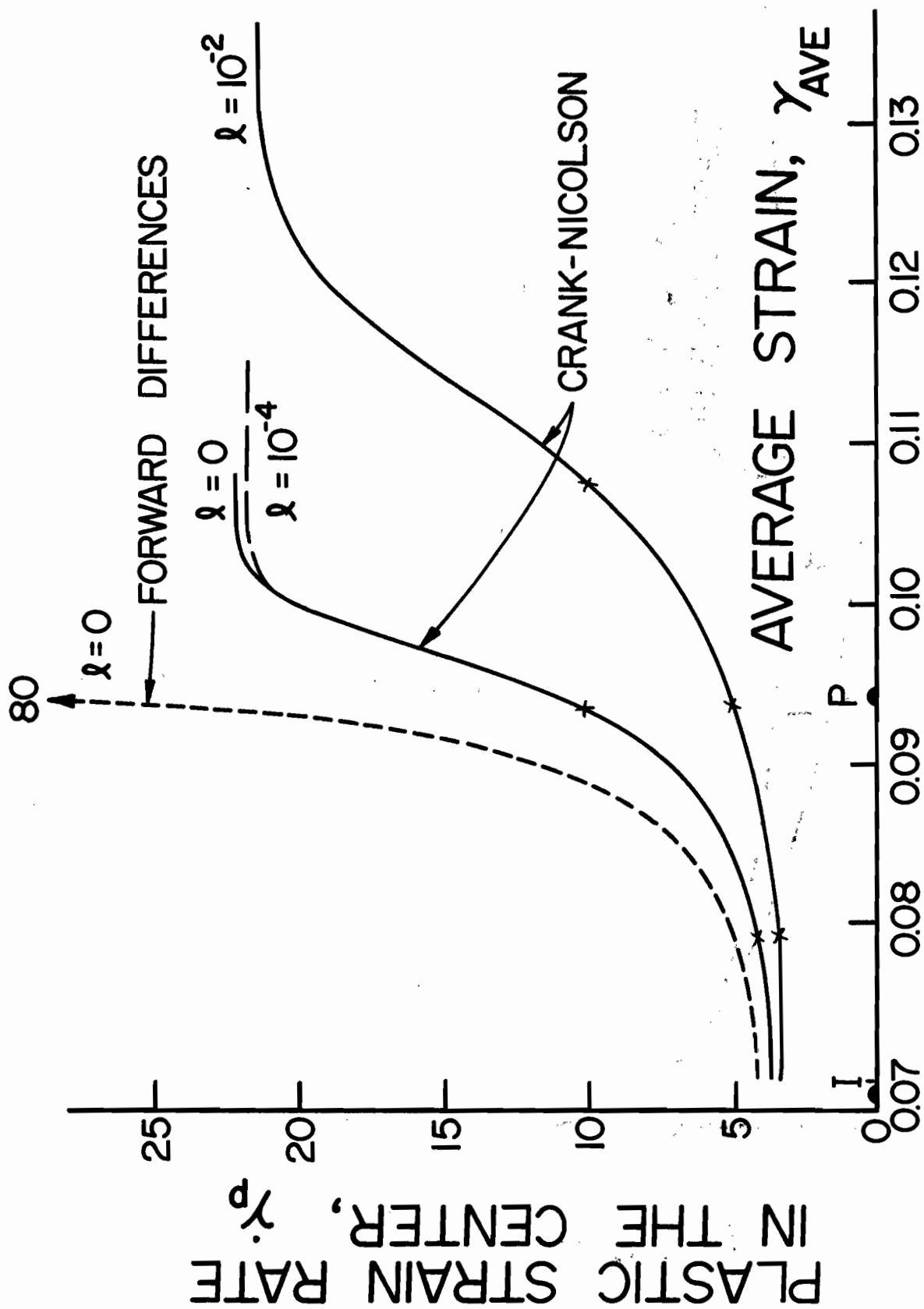


Figure 2. Plastic strain rate in the center of the band with a temperature perturbation.

exactly equal to increments of the average applied strain, so the curve may be interpreted equally well as a time plot. After a brief interval during which the field variables regain their essential balance, the central plastic strain rate begins a slow but accelerating climb. Eventually it turns up rather sharply for  $\ell = 0$  or  $10^{-4}$  and somewhat less sharply for  $\ell = 10^{-2}$ , the first two cases being virtually indistinguishable. Also, shown is the result from previous calculations<sup>2</sup> with  $\ell = 0$ , where the strain rate increases even more dramatically. The delay in the response for the present case relative to the previous one with  $\ell = 0$  is probably due to a nonphysical damping, which is introduced by the Crank-Nicolson scheme as compared to the forward difference method. The result for  $\ell = 10^{-2}$  relative to the other two cases shows the same stiffening effect due to the material length  $\ell$  that was reported in Ref. 2. It is clear that the rate of increase of plastic strain rate can be substantially retarded if  $\ell$  is large enough.

All cases calculated so far show the development of a late stage plateau, but the computed value is a numerical artifact and is not a physical result. Since  $v = 1$  at the boundary  $Y = 1$ , it follows that

$$\int_0^1 \dot{\gamma} dY = \int_0^1 v_{,Y} dY = 1 \quad .$$

As shown in Figure 3, the plastic strain rate builds up in the center, but it decreases in the outer region. In the plateau region of the calculations, the plastic strain rate is nonzero at the center but falls to zero at  $Y = 0.1$ . With linear interpolation the nonzero part of the distribution is triangular, so the level of the plateau is effectively caused by the length scale that is introduced through the computational grid. In the previous results<sup>1,2</sup> a more complicated interpolation scheme and a finer grid were used, which allowed the plateau to be delayed until the plastic rate reached approximately 80, as indicated in the figure. Although the level of the plateau is nonphysical, the fact that it is very likely fixed by the length scale of the grid suggest that one might expect a true plateau to develop where the level would be determined by the physical length scales of the problem. Two such physical lengths, one arising from thermal conductivity and one from viscous stress effects, were identified in Ref. 1 and the parameter  $\ell$  is a possible third one. All three length scales may be very small and beyond convenient numerical resolution.

The cross plots of plastic strain rate at increasing values of average strain, as shown in Figure 3, are taken well before the plateau is reached, and so should be accurately representative of the progressive localization that occurs. The five crosses on the curves in Figure 2 correspond to the five curves in Figure 3. As the deformation continues, the plastic strain rate builds up in the center, but decreases in the outer regions. The relative stiffening of the dipolar material can be seen clearly in Figure 3 as well. For example, when the average strain reaches 0.093, the dipolar case with  $\ell = 10^{-2}$  has reached only half the value for the cases  $\ell = 0$  or  $10^{-4}$ , and obviously continues to develop at a much slower rate. Since the peak in plastic strain rate is lower for larger values of  $\ell$ , naturally the distribution is broader and the rate falls more slowly in the outer regions, as well.

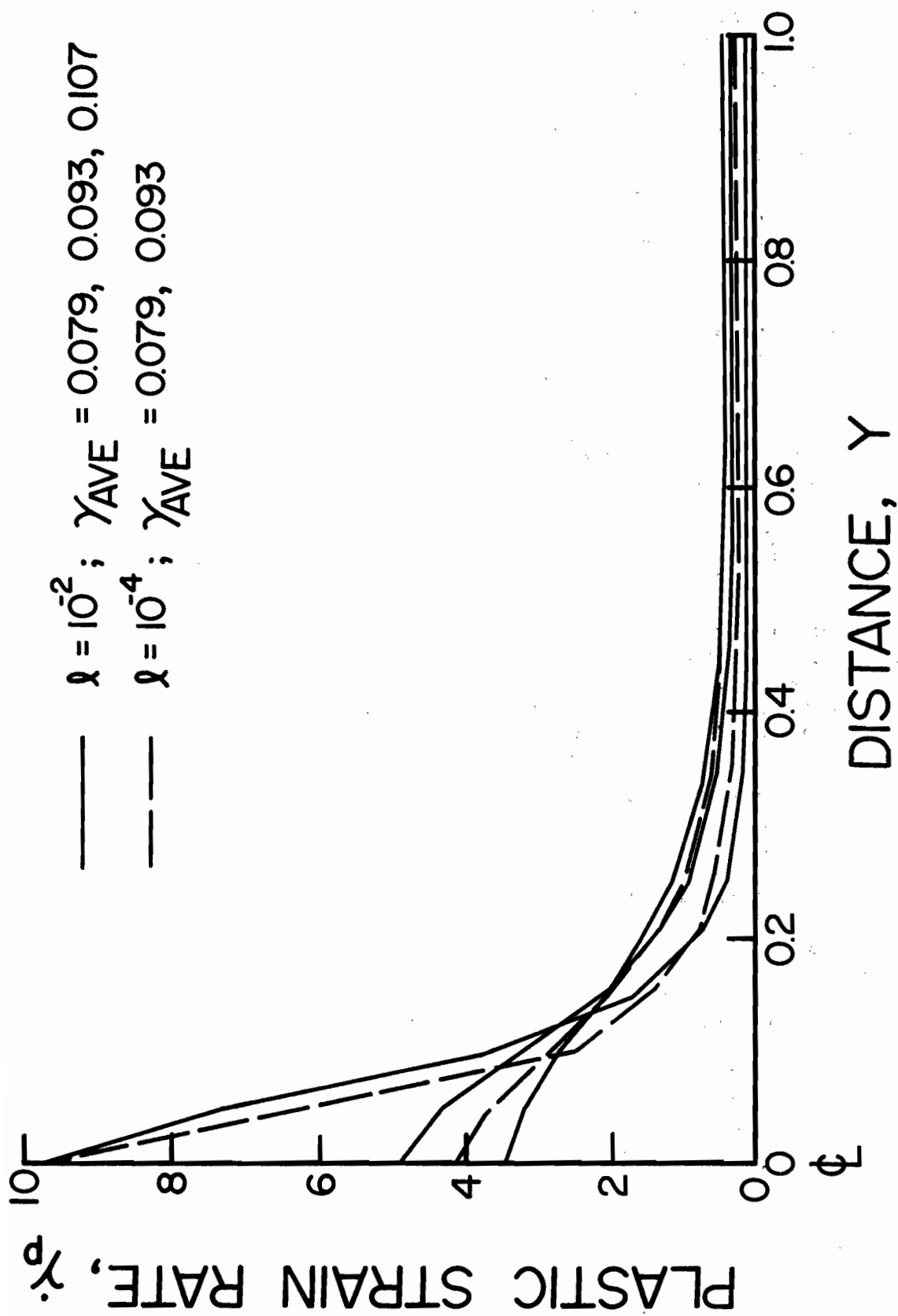


Figure 3. Cross plots of plastic strain for increasing deformation.

Temperature plots are not shown, but the results are similar to the previous calculations. At first the temperature follows the path of the homogeneous case quite closely, but as the deformation localizes so does the temperature distribution with a peak forming in the center and a plateau forming in the outer regions as the plastic heating falls to zero.

In all calculations so far the case for  $\ell = 10^{-4}$  shows essentially no difference from the simple material. The reason for this is shown dramatically in Figure 4, which shows the dipolar stress distribution at several values of time. The assumed symmetry of the problem requires that the dipolar stress be an odd function of  $Y$ , and hence that it vanish at  $Y = 0$ . The peak of the distribution for  $\ell = 10^{-2}$  lies near  $Y = 0.2$  and moves somewhat toward the center for increasing time. The dipolar distribution for  $\ell = 10^{-4}$  shows a similar shape, but now the peak value is only about 2% of the peak value for  $\ell = 10^{-2}$  at the same time. For the smaller value of  $\ell$  the dipolar effect is so weak that it has no effect on the calculations prior to the formation of the false plateau.

Figure 5 shows the computed values of shear stress as a function of average applied strain. At first the stress for each of the perturbed cases follows the homogeneous case quite closely, but eventually it deviates markedly. The stress remains nearly constant through the cross section at all times until the strain rate accelerates sharply upwards. Then the stress begins to fall, first in the center and then in the outer regions. The start of the drop in stress is clearly evident in the computed results, although in every case the curves have been drawn past the probable limit of validity (the tick mark on the curve). Here again the stiffening effect of the dipolar stress is evident in the delay and rate of departure from the homogeneous case. It is also interesting to note that even though the dipolar stress attains significant values, and the stiffening effect is clearly evident in the distribution of plastic strain, there is little difference between the shear stress  $s$  and the traction  $\tau$ , as might have been expected from equation (3).

## V. DISCUSSION AND CONCLUSIONS

In this paper a formulation has been given for shearing of thermo/viscoplastic dipolar material with heat conduction. Because of thermal softening, the stress at a point in the material may decrease with further straining, and so the material may tend to localize in the same manner as for a simple material. The dipolar, or gradient, effect has been added because large strain and temperature gradients form in the localized region. It has been found that this additional constitutive property has a stiffening effect relative to a simple material. That is, for the same perturbation the onset of localization is delayed and the rate of growth of the perturbation decreases with increasing dipolar strength. It has been found that the Crank-Nicolson scheme for stepping forward in time allows a much larger time step to be used than the simple forward difference method, but it also seems to introduce some artificial damping.



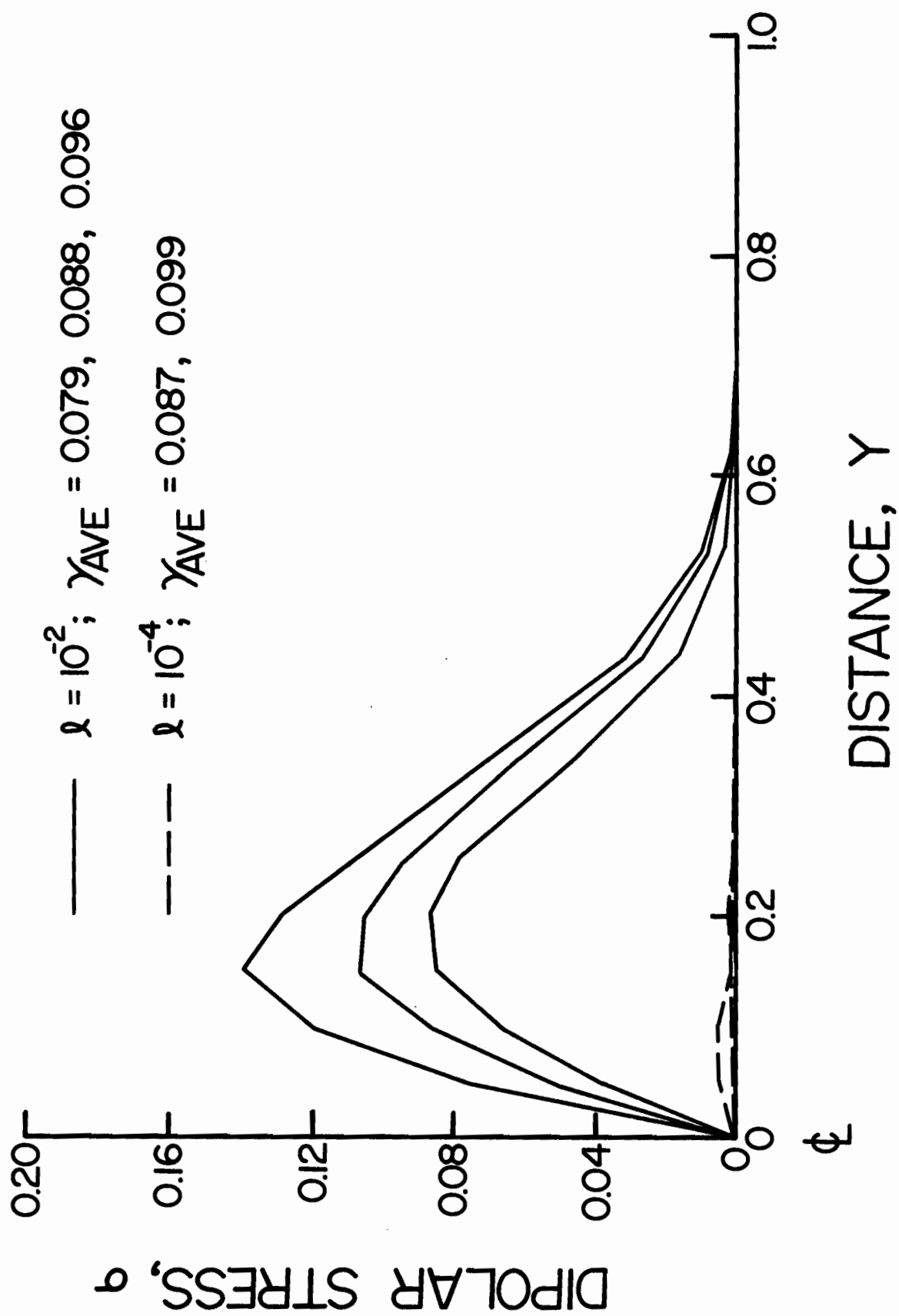
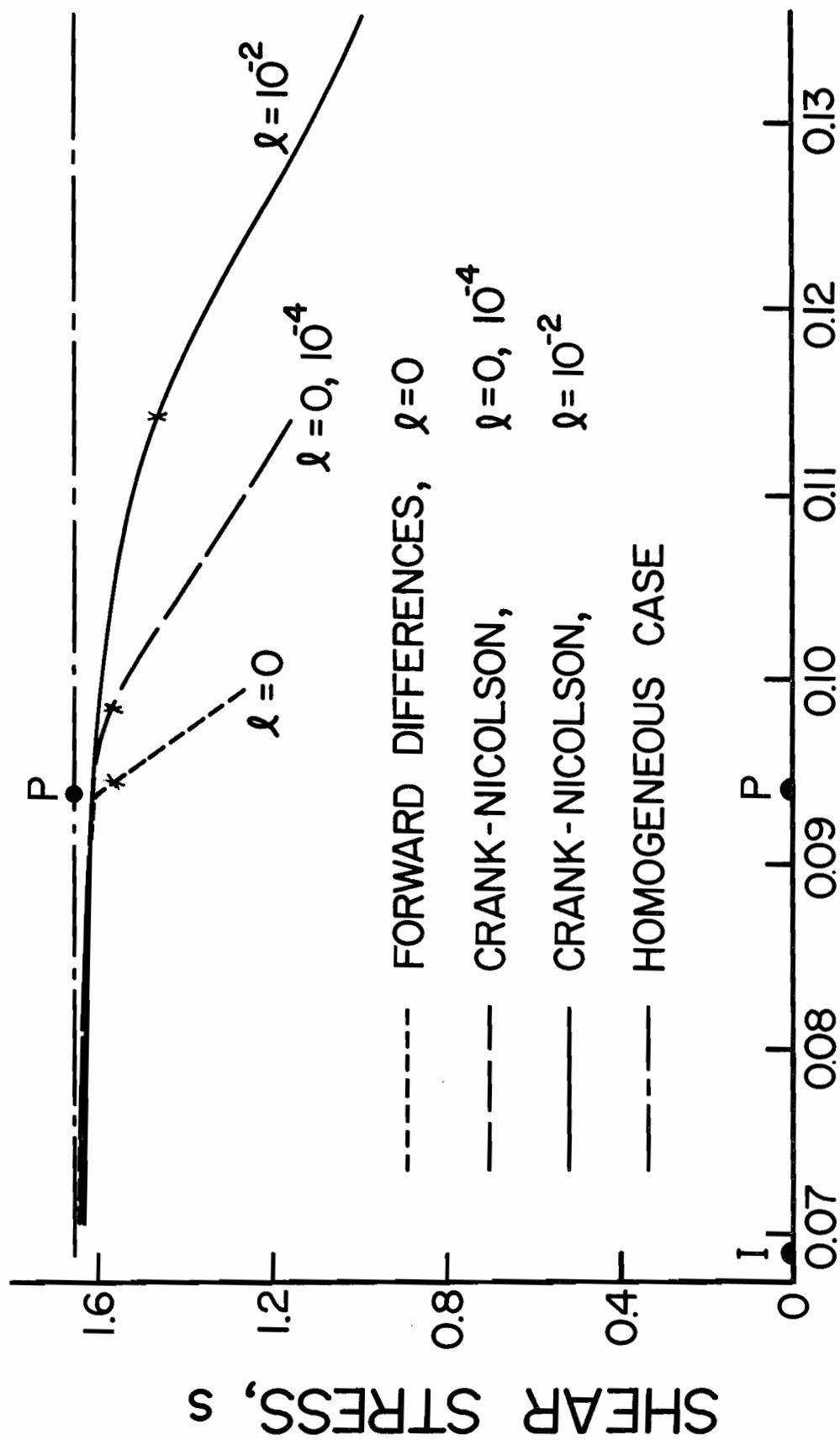


Figure 4. Cross plots of dipolar stress for increasing deformation.



AVERAGE STRAIN,  $\gamma_{AVE}$

Figure 5. Stress in a shear band.

#### REFERENCES

1. Wright, T. W. and Batra, R. C., The Initiation and Growth of Adiabatic Shear Bands. *Int. J. Plasticity* 1, 205-212, 1985.
2. Wright, T. W. and Batra, R. C., Further Results on the Initiation and Growth of Adiabatic Shear Bands at High Strain Rates, *J. de Physique* 45, Coll. C5, 323-330, 1985.
3. Moss, G. L., Shear Strains, Strain Rates and Temperature Changes in Adiabatic Shear Bands, In Shock Waves and High-strain Rate Phenomena in Metals, Meyers, M. A.; Murr, L. E. (eds.). New York; Plenum Press, 1981.
4. Green, A. E., McInnis, B. C., and Naghdi, P. M., Elastic-Plastic Continua With Simple Force Dipole. *Int. J. Eng. Sci* 6, 373-394, 1968.

# DISTRIBUTION LIST

<u>No. of</u> <u>Copies</u>	<u>Organization</u>	<u>No. of</u> <u>Copies</u>	<u>Organization</u>
12	Administrator Defense Technical Info Center ATTN: DTIC-DDA Cameron Station Alexandria, VA 22304-6145	3	Commander U.S. Army Armament Research, Development and Engineering Center ATTN: SMCAR-SC, J. D. Corrie J. Beetle E. Bloore Dover, NJ 07801-5001
4	Director Defense Advanced Research Projects Agency ATTN: Tech Info Dr. E. Van Reuth Dr. G. Farnum Dr. B. Wilcox 1400 Wilson Boulevard Arlington, VA 22209	1	Commander U.S. Army ARDEC ATTN: SMCAR-TDC Dover, NJ 07801
1	Deputy Assistant Secretary of the Army (R&D) Department of the Army Washington, DC 20310	1	Commander U.S. Army Armament Research, Development and Engineering Center ATTN: SMCAR-MSI Dover, NJ 07801-5001
1	HQDA DAMA-ART-M Washington, DC 20310	1	Commander Benet Weapons Laboratory ATTN: Dr. E. Schneider Watervliet, NY 12189
1	Commander U.S. Army War College ATTN: Lib Carlisle Barracks, PA 17013	1	Director U.S. AMCCOM ARDEC CCAC Benet Weapons Laboratory ATTN: SMCAR-LCB-TL Watervliet, NY 12189-4050
1	Commander U.S. Army Command and General Staff College ATTN: Archives Fort Leavenworth, KS 66027	1	Commander U.S. Army Armament, Munitions and Chemical Command ATTN: SMCAR-ESP-L Rock Island, IL 61299-7300
1	Commander U.S. Army Materiel Command ATTN: AMCDRA-ST 5001 Eisenhower Avenue Alexandria, VA 22333-0001	1	Commander U.S. Army Aviation Systems Command ATTN: AMSAV-E 4300 Goodfellow Boulevard St. Louis, MO 63120-1798
1	Commander U.S. Army Armament Research, Development and Engineering Center ATTN: SMCAR-LCA, T. Davidson Dover, NJ 07801-5001	1	Commander Armament R&D Center US Army AMCCOM ATTN: SMCAR-TSS Dover, NJ 07801

# DISTRIBUTION LIST

<u>No. of</u> <u>Copies</u>	<u>Organization</u>	<u>No. of</u> <u>Copies</u>	<u>Organization</u>
1	Director U.S. Army Air Mobility Research and Development Laboratory Ames Research Center Moffett Field, CA 94035-1099	2	Commander U.S. Army Mobility Equipment Research & Development Command ATTN: DRDME-WC DRSME-RZT Fort Belvoir, VA 22060
1	Commander U.S. Army Communications - Electronics Command ATTN: AMSEL-ED Fort Monmouth, NJ 07703-5301	1	Commander U.S. Army Natick Research and Development Center ATTN: DRXRE, Dr. D. Sieling Natick, MA 01762
1	Commander ERADCOM Technical Library ATTN: DELSD-L (Reports Section) Fort Monmouth, NJ 07703-5301	1	Commander U.S. Army Tank Automotive Command ATTN: AMSTA-TSL Warren, MI 48397-5000
1	Commander U.S. Army Harry Diamond Laboratory ATTN: SLCHD-TA-L 2800 Powder Mill Road Adelphi, MD 20783	1	Commander USAG ATTN: Technical Library Fort Huachuca, AZ 85613-6000
1	Commander MICOM Research, Development and Engineering Center ATTN: AMSMI-RD Redstone Arsenal, AL 35898-5500	1	Commander U.S. Army Development and Employment Agency ATTN: MODE- TED-SAB Fort Lewis, WA 98433
1	Director Missile and Space Intelligence Center ATTN: AIAM-S-YDL Redstone Arsenal, AL 35898-5500	3	Commander U.S. Army Laboratory Command Materials Technology Laboratory ATTN: SLCMT-T, J. Mescall SLCMT-T, R. Shea SLCMT-H, S.C. Chou Watertown, MA 02172-0001
3	Director BMD Advanced Technology Center ATTN: ATC-T, M. Capps ATC-M, S. Brockway ATC-RN, P. Boyd P.O. Box 1500 Huntsville, AL 35807	1	Director U.S. Army TRADOC Analysis Center ATTN: ATAA-SL White Sands Missile Range, 88002-5502

# DISTRIBUTION LIST

<u>No. of</u> <u>Copies</u>	<u>Organization</u>	<u>No. of</u> <u>Copies</u>	<u>Organization</u>
1	Commandant U.S. Army Infantry School ATTN: ATSH-CD-CS-OR Fort Benning, GA 31905-5400	3	Commander Naval Surface Weapons Center ATTN: Dr. W. H. Holt Dr. W. Mock Tech Lib Dahlgren, VA 22448-5000
1	Director U.S. Army Advanced BMD Technology Center ATTN: CRDABH-5, W. Loomis P. O. Box 1500, West Station Huntsville, AL 35807	3	Commander Naval Surface Weapons Center ATTN: Dr. R. Crowe Code R32, Dr. S. Fishman Code X211, Lib Silver Spring, MD 20902-5000
3	Commander U.S. Army Research Office ATTN: Dr. E. Saibel Dr. G. Mayer Dr. J. Chandra P. O. Box 12211 Research Triangle Park, NC 27709	1	Commander and Director US Naval Electronics Laboratory San Diego, CA 92152
2	Commander U.S. Army Research and Standardization Group (Europe) ATTN: Dr. J. Wu Dr. F. Oertel Box 65 FPO NY 09510	5	Air Force Armament Laboratory ATTN: AFATL/DLODL  J. Foster John Collins Joe Smith Guy Spitale Eglin AFB, FL 32542-5438
3	Office of Naval Research Department of the Navy ATTN: Dr. Y. Rajapakse Dr. A. Tucker Dr. A. Kushner Washington, DC 20360	1	RADC (EMTLD, Lib) Griffiss AFB, NY 13440
3	Commander U.S. Naval Air Systems Command ATTN: AIR-604 Washington, DC 20360	1	AUL (3T-AUL-60-118) Maxwell AFB, AL 36112
1	Commander Naval Sea Systems Command ATTN: Code SEA 62D Department of the Navy Washington, DC 20362-5101	1	Air Force Wright Aeronautical Laboratories Air Force Systems Command Materials Laboratory ATTN: Dr. Theodore Nicholas Wright-Patterson AFB, OH 45433
		1	AFWL/SUL Kirtland AFB, NM 87117

# DISTRIBUTION LIST

<u>No. of</u> <u>Copies</u>	<u>Organization</u>	<u>No. of</u> <u>Copies</u>	<u>Organization</u>
1	Air Force Wright Aeronautical Laboratories Air Force Systems Command Materials Laboratory ATTN: Dr. John P. Henderson Wright-Patterson AFB, OH 45433	1	Director Jet Propulsion Laboratory ATTN: Lib (TDS) 4800 Oak Grove Drive Pasadena, CA 91103
1	Director Environmental Science Service Administration US Department of Commerce Boulder, CO 80302	1	National Bureau of Standards ATTN: Dr. Timothy Burns Technology Building, Rm A151 Gaithersburg, MD 20899
1	Director Lawrence Livermore Laboratory ATTN: Dr. M. L. Wilkins P. O. Box 808 Livermore, CA 94550	1	A.R.A.P. Group Titan Systems, Inc. ATTN: Ray Gogolewski 1800 Old Meadow Rd., #114 McLean, VA 22102
8	Sandia National Laboratories ATTN: Dr. L. Davison Dr. P. Chen Dr. L. Bertholf Dr. W. Herrmann Dr. J. Nunziato Dr. S. Passman Dr. E. Dunn Dr. M. Forrestal P. O. Box 5800 Albuquerque, NM 87185-5800	1	ETA Corporation ATTN: Dr. D. L. Mykkanen P. O. Box 6625 Orange, CA 92667
1	Sandia National Laboratories ATTN: Dr. D. Bamman Livermore, CA 94550	1	Forestal Research Center Aeronautical Engineering Lab. Princeton University ATTN: Dr. A. Eringen Princeton, NJ 08540
1	Director National Aeronautics and Space Administration Lyndon B. Johnson Space Center ATTN: Lib Houston, TX 77058	1	Honeywell, Inc. Defense Systems Division ATTN: Dr. Gordon Johnson 600 Second Street, NE Hopkins, MN 55343
		2	Orlando Technology, Inc. ATTN: Dr. Daniel Matuska Dr. John J. Osborn P. O. Box 855 Shalimar, FL 32579

# DISTRIBUTION LIST

<u>No. of</u> <u>Copies</u>	<u>Organization</u>	<u>No. of</u> <u>Copies</u>	<u>Organization</u>
6	SRI International ATTN: Dr. Donald R. Curran Dr. Donald A. Shockey Dr. Lynn Seaman Mr. D. Erlich Dr. A. Florence Dr. R. Caligiuri 333 Ravenswood Avenue Menlo Park, CA 94025	3	Rensselaer Polytechnic Institute ATTN: Prof. E. H. Lee Prof. E. Kreml Prof. J. Flaherty Troy, NY 12181
1	Systems Planning Corporation ATTN: Mr. T. Hafer 1500 Wilson Boulevard Arlington, VA 22209	1	Southwest Research Institute Department of Mechanical Sciences ATTN: Dr. U. Lindholm 8500 Culebra Road San Antonio, TX 78228
1	Terra-Tek, Inc. ATTN: Dr. Arfon Jones 420 Wahara Way University Research Park Salt Lake City, UT 84108	5	Brown University Division of Engineering ATTN: Prof. R. Clifton Prof. H. Kolsky Prof. L. B. Freund Prof. A. Needleman Prof. R. Asaro Providence, RI 02912
2	California Institute of Technology Division of Engineering and Applied Science ATTN: Dr. E. Sternberg Dr. J. Knowles Pasadena, CA 91102	1	Brown University Division of Applied Mathematics ATTN: Prof. C. Dafermos Providence, RI 02912
1	Denver Research Institute University of Denver ATTN: Dr. R. Recht P. O. Box 10127 Denver, CO 80210	3	Carnegie-Mellon University Department of Mathematics ATTN: Dr. D. Owen Dr. M. E. Gurtin Dr. B. D. Coleman Pittsburgh, PA 15213
1	Massachusetts Institute of Technology ATTN: Dr. R. Probststein 77 Massachusetts Avenue Cambridge, MA 02139	7	Cornell University Department of Theoretical and Applied Mechanics ATTN: Dr. Y. H. Pao Dr. G. S. S. Ludford Dr. A. Ruoff Dr. J. Jenkins Dr. R. Lance Dr. F. Moon Dr. E. Hart Ithaca, NY 14850
1	Massachusetts Institute of Technology Department of Mechanical Engineering ATTN: Prof. L. Anand Cambridge, MA 02139		



# DISTRIBUTION LIST

<u>No. of Copies</u>	<u>Organization</u>	<u>No. of Copies</u>	<u>Organization</u>
2	Harvard University Division of Engineering and Applied Physics ATTN: Prof. J. R. Rice Prof. J. Hutchinson Cambridge, MA 02138	1	Southern Methodist University Solid Mechanics Division ATTN: Prof. H. Watson Dallas, TX 75221
2	Iowa State University Engineering Research Laboratory ATTN: Dr. A. Sedov Dr. G. Nariboli Ames, IA 50010	1	Temple University College of Engineering Tech. ATTN: Dr. R. Haythornthwaite Dean Philadelphia, PA 19122
2	Lehigh University Center for the Application of Mathematics ATTN: Dr. E. Varley Dr. R. Rivlin Bethlehem, PA 18015	5	The Johns Hopkins University ATTN: Prof. R. B. Pond, Sr. Prof. R. Green Prof. W. Sharpe Prof. J. F. Bell Prof. C. A. Truesdell 34th and Charles Streets Baltimore, MD 21218
1	New York University Department of Mathematics ATTN: Dr. J. Keller University Heights New York, NY 10053	1	Tulane University Department of Mechanical Engineering ATTN: Dr. S. Cowin New Orleans, LA 70112
1	North Carolina State University Department of Civil Engineering ATTN: Prof. Y. Horie Raleigh, NC 27607	3	University of California Department of Mechanical Engineering ATTN: Dr. M. Carroll Dr. W. Goldsmith Dr. P. Naghdi Berkeley, CA 94704
1	Pennsylvania State University Engineering Mechanical Dept. ATTN: Prof. N. Davids University Park, PA 16502	1	University of California Dept of Aerospace and Mechanical Engineering Science ATTN: Dr. Y. C. Fung P. O. Box 109 La Jolla, CA 92037
1	Rice University ATTN: Dr. C. C. Wang P. O. Box 1892 Houston, TX 77001		

# DISTRIBUTION LIST

<u>No. of Copies</u>	<u>Organization</u>	<u>No. of Copies</u>	<u>Organization</u>
1	University of California Department of Mechanics ATTN: Dr. R. Stern 504 Hilgard Avenue Los Angeles, CA 90024	2	University of Houston Department of Mechanical Engineering ATTN: Dr. T. Wheeler Dr. R. Nachlinger Houston, TX 77004
1	University of California at Santa Barbara Department of Mechanical Engineering ATTN: Prof. T. P. Mitchel Santa Barbara, CA 93106	2	University of Illinois Department of Theoretical and Applied Mechanics ATTN: Dr. D. Carlson Prof. D. Scott Stewart Urbana, IL 61801
1	University of California at Santa Barbara Department of Materials Science ATTN: Prof. A. G. Evans Santa Barbara, CA 93106	2	University of Illinois at Chicago Circle College of Engineering Department of Engineering, Mechanics, and Metallurgy ATTN: Prof. T.C.T. Ting Prof. D. Krajcinovic P. O. Box 4348 Chicago, IL 60680
1	University of California at San Diego Department of Mechanical Engineering ATTN: Prof. S. Nemat Nassar La Jolla, CA 92093	2	University of Kentucky Department of Engineering Mechanics ATTN: Dr. M. Beatty Prof. O. Dillon, Jr. Lexington, KY 40506
2	University of Delaware Department of Mechanical and Aerospace Engineering ATTN: Dr. Minoru Taya Prof. J. Vinson Newark, DE 19711	1	University of Kentucky School of Engineering ATTN: Dean R. M. Bowen Lexington, KY 40506
3	University of Florida Department of Engineering Science and Mechanics ATTN: Prof. L. Malvern Prof. D. Drucker Prof. E. Walsh Gainesville, FL 32601	2	University of Maryland Department of Mathematics ATTN: Prof. S. Antman Prof. T. P. Liu College Park, MD 20742

# DISTRIBUTION LIST

<u>No. of</u> <u>Copies</u>	<u>Organization</u>	<u>No. of</u> <u>Copies</u>	<u>Organization</u>
3	University of Minnesota Department of Engineering Mechanics ATTN: Prof. J. L. Erickson Prof. R. Fosdick Prof. R. James Minneapolis, MN 55455	1	University of Wyoming Department of Mathematics ATTN: Prof. R. E. Ewing P. O. Box 3036 University Station Laramie, WY 82070
1	University of Missouri-Rolla Department of Engineering Mechanics ATTN: Prof. R. C. Batra Rolla, MO 65401-0249	3	Washington State University Department of Physics ATTN: Prof. R. Fowles Prof. G. Duvall Prof. Y. Gupta Pullman, WA 99163
2	University of Oklahoma School of Aerospace, Mechanical and Nuclear Engineering ATTN: Prof. Akhtar S. Khan Prof. Charles W. Bert Norman, Oklahoma 73019	2	Yale University ATTN: Dr. B.-T. Chu Dr. E. Onat 400 Temple Street New Haven, CT 96520
1	University of Pennsylvania Towne School of Civil and Mechanical Engineering ATTN: Prof. Z. Hashin Philadelphia, PA 19105	<u>Aberdeen Proving Ground</u>	
4	University of Texas Department of Engineering Mechanics ATTN: Dr. M. Stern Dr. M. Bedford Prof. Ripperger Dr. J. T. Oden Austin, TX 78712	Dir, USAMSAA ATTN: AMXSY-D AMXSY-MP, H. Cohen Cdr, USATECOM ATTN: AMSTE-SI-F Cdr, CRDC, AMCCOM ATTN: SMCCR-RSP-A SMCCR-MU SMCCR-SPS-IL	
1	University of Washington Department of Aeronautics and Astronautics ATTN: Dr. Ian M. Fyfe 206 Guggenheim Hall Seattle, WA 98195	10	Central Intelligence Agency Office of Central Reference Dissemination Branch Room GE-47 HQS Washington, DC 20502